

Lattice simulations of a gauge theory with mixed adjoint-fundamental matter

Georg Bergner^{*}

*University of Jena, Institute for Theoretical Physics, Max-Wien-Platz 1, D-07743 Jena, Germany
and University of Münster, Institute for Theoretical Physics, Wilhelm-Klemm-Str. 9,
D-48149 Münster, Germany*

Stefano Piemonte[†]

Institute for Theoretical Physics, University of Regensburg, D-93040 Regensburg, Germany



(Received 16 September 2020; accepted 4 December 2020; published 4 January 2021)

In this paper, we summarize our efforts in simulating Yang-Mills theories coupled to matter fields transforming under the fundamental and adjoint representations of the gauge group. In the context of composite Higgs scenarios, gauge theories with mixed representation fields have been suggested to describe the fundamental interactions well beyond the electroweak unification scale, and they are also closely related to supersymmetric QCD. In addition, they are studied as deformations of theories with pure adjoint matter in the context of adiabatic continuity. We provide some first results for bare parameter tuning and interdependence of the two representations. We also investigate how the chiral symmetry breaking or a conformal scenario can be realized and checked in such theories.

DOI: [10.1103/PhysRevD.103.014503](https://doi.org/10.1103/PhysRevD.103.014503)

I. GAUGE THEORIES WITH ADJOINT AND FUNDAMENTAL FERMIONS

In the last two decades, there has been a substantial effort to extend lattice Monte Carlo simulations from quantum chromodynamics (QCD) toward the full landscape of gauge theories including different numbers of fermion fields transforming in the fundamental representation of the gauge group. Higher fermion representations have been also considered, most notably the adjoint representation of SU(2) and SU(3), and the sextet representation of SU(3). The motivations for these studies have been the search for an extension of the Standard Model or the consideration of supersymmetric gauge theories. The first studies of gauge theories coupled to fermions in two different representations have been published very recently [1–6]. Such a setup enhances substantially the possibilities for model building and investigations of general theoretical questions. Our study of a mixed representation setup with an SU(2) gauge theory coupled to two Dirac fermions in the fundamental and one Majorana fermion in the adjoint representation has several motivations.

The first aim is an exploratory study toward the investigations of supersymmetric QCD (SQCD). SQCD is described by SU(N_c) gauge fields coupled to fermionic gluinos in the adjoint representation of the gauge group as well as N_f fermionic quark fields and scalar squark fields in the fundamental representation. Depending on N_c and N_f , different phases of the theory are expected. In particular, there are predictions for the appearance of an IR conformal fixed point in this parameter space. There have been several attempts toward a simulation of SQCD on the lattice [7–10], but so far no real and complete investigation has been possible. Since there has not been much experience with numerical simulations of mixed representations, it is important to understand first the theory without scalar fields, as a first step toward SQCD.

A second aim is related to possible composite Higgs theories [11]. Theories with fermions in higher representations have been already investigated in this context. One of the most famous examples is minimal walking technicolor (MWT), an SU(2) gauge theory with $N_f = 2$ Dirac fermions in the adjoint representation. As shown by numerical investigations, the mass anomalous dimension at the IR fixed point of this theory is quite small, which makes it less favorable for a Standard Model extension [12–14].¹ Theories with smaller N_f lead to a larger value of

^{*}georg.bergner@uni-jena.de

[†]stefano.piemonte@ur.de

Published by the American Physical Society under the terms of the Creative Commons Attribution 4.0 International license. Further distribution of this work must maintain attribution to the author(s) and the published article's title, journal citation, and DOI. Funded by SCOAP³.

¹Early simulations of SU(2) with fermions in the adjoint representation can be found in [15] and in [16] for the fundamental representation.

the mass anomalous dimension [17,18], but they do not provide the right particle content for the coupling to the Standard Model. One possible way out is to combine different representations. The matter content for a coupling of the SU(2) gauge theory to the Standard Model are two fundamental fermions and the theory is driven toward the conformal or walking limit by additional adjoint fermion flavors. The adjoint matter is not charged under the gauge groups of the Standard Model. This minimizes the matter content of a possible Standard Model extension compared to an approach with only fundamental matter since the adjoint representation requires a smaller number of flavors to reach near conformality.

The theory with two fundamental and one adjoint Dirac flavor, the so-called ultraminimal walking technicolor (UMWT), has been suggested as a strongly interacting completion of the Standard Model [19].² Due to the relation to SQCD, we are considering here only one Majorana fermion in the adjoint representation. This might nevertheless already be sufficient for near conformality since the analysis of the theory has so far only been based on perturbative estimates. The theory can, furthermore, be considered as a deformation SU(2) gauge theory with two fermions in the fundamental representation, which has been considered in several investigations as a composite Higgs model; see, for example, numerical studies in [22–25].

Another relation of our investigations in the context of composite Higgs is the approach of a fine grained control of the running of the gauge coupling by different mass scales. This has been suggested and investigated for theories with a large number of flavors in the fundamental representation of SU(3) [26–28]. The fermion fields have been split in a set of $(N_f)_h$ heavy and $(N_f)_l$ light fermions. However, this appears more natural in the context of mixed representations as there is no symmetry suggesting an equality of the masses of the different representations. Our studies might also provide additional insights for the general investigations with multiple fermion representations, which appear in the context of composite Higgs theories and partial compositeness [29]. There are so far only a limited number of lattice studies in this context [1,2,6].

The third line of motivation is related to a predicted analytic continuity between confinement of strongly coupled gauge theories and confinement in a semiclassical small circle regime. This provides a better analytic control in investigations of the relevance of nonperturbative semiclassical contributions in the confinement mechanism. The phenomenon is well understood in supersymmetric Yang-Mills (SYM) theory and also confirmed by numerical simulations [30,31]. Theoretical studies have been based on the assumption that this can be extended toward gauge theories with a larger number of adjoint fermion flavors

²The consideration of mixed representations has been extended and generalized in [20,21].

than the one Majorana fermion corresponding to SYM. It is difficult to verify these findings since already at one Dirac flavor, the theory becomes nearly conformal. The extension of SYM by fermion fields in the fundamental representation enlarges the space of possible applications for analytic continuity [32,33]. It might also help to relate the SYM confinement with the confinement of QCD in a continuous way.

The current study represents the essential first step for all of these investigations, being an exploration of the parameter space spanned by the two mass parameters of the different representations and the gauge coupling. The study of the scaling of the meson mass spectrum close to the chiral limit provides a clear picture helping to distinguish the signals of a chiral symmetry breaking scenario from a conformal theory. In particular, the main target of the present investigations is the deformation of the spectrum of lowest mesonic states induced by the addition of fermions in a different representation. As a first step, we aim to identify possible unphysical bulk phases, which appear for higher representations and in particular in the context of near conformal theories. An important cross-check of our current first studies is also the connection to pure adjoint and fundamental limits.

II. A THEORY WITH TWO DIFFERENT FERMION REPRESENTATIONS ON THE LATTICE

The first step for Monte Carlo simulations is the lattice discretization of the continuum action. In our numerical simulations, the gauge part of the lattice action is represented by the Wilson gauge action built from plaquettes U_p of link variables U in fundamental representation of SU(N_c). The fermionic part comprises a Dirac-Wilson clover improved action for $N_f^{(F)}$ fermions in the fundamental and $N_f^{(A)}$ fermions in the adjoint representation. In its basic form, the complete lattice action reads

$$\mathcal{S}_L = \beta \sum_p \left(1 - \frac{1}{N_c} \text{Re tr} U_p \right) + \sum_{x,y} \sum_{n_f=1}^{N_f^{(F)}} \bar{\psi}_x^{n_f} (D_w^{(F)})_{xy} \psi_y^{n_f} + \sum_{x,y} \sum_{n_f=1}^{N_f^{(A)}} \bar{\psi}_x^{n_f} (D_w^{(A)})_{xy} \psi_y^{n_f}, \quad (1)$$

where $D_w^{(F)}$ ($D_w^{(A)}$) is the clover Wilson-Dirac operator in the fundamental (adjoint) representation. These operators depend on the hopping parameter κ_F (κ_A), which is related to the bare fermion mass m_0 in the respective representation via $\kappa = 1/(2m_0 + 8)$. Like in our previous studies, the link fields in $D_w^{(A)}$ are converted to the adjoint representation. The two clover parameters have been tuned by a one-loop perturbative calculation [34], that has already provided

significant improvements in our previous studies of pure SYM.

Our simulation program allows flexible simulation for an arbitrary number of fermions in the adjoint and fundamental representation of an $SU(N_c)$ gauge group. In the current work, we consider one adjoint Majorana fermion, effectively $N_f^{(A)} = \frac{1}{2}$, simulated with the rational hybrid Monte Carlo algorithm (RHMC), and two degenerate flavors in the fundamental representation ($N_f^{(F)} = 2$) which are represented by the standard hybrid Monte Carlo (HMC) algorithm.

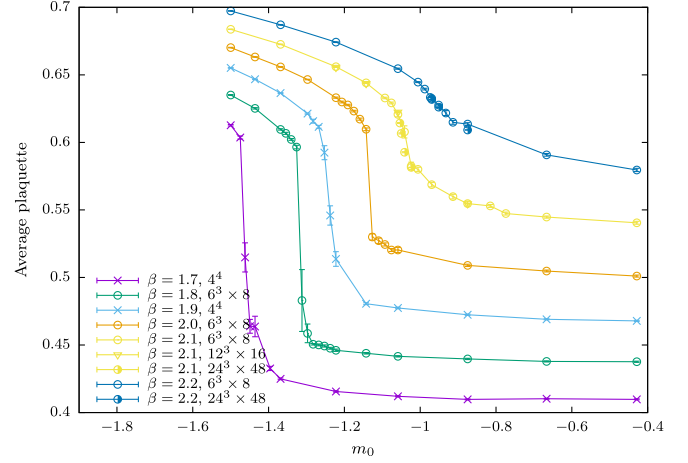
The tuning of the RHMC algorithm has been done based on our experience with simulations of SYM. In SYM, rather precise rational approximations have been needed for simulations close enough to the chiral limit. Despite the fact that also heavier masses have been considered here, we have still kept a rather high order approximations in most of the simulations. In the HMC, different force contributions for each fermion representation and for the gauge action have to be considered. Our program allows to have multiple time scales for the integration and we have adjusted these parameters according to the relevance of the different force contributions.

III. PHASE TRANSITIONS AT STRONG COUPLING

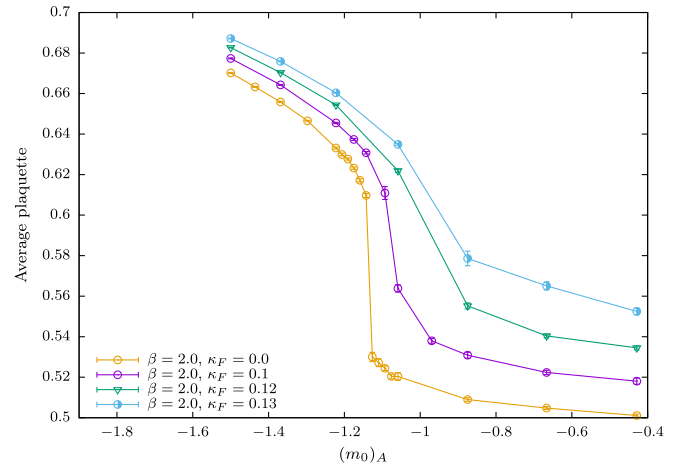
In a first study of the theory, we map out the phase diagram on small lattices to identify possible unphysical bulk phases appearing in the context of IR conformal theories. In the bare parameter space of these theories, the strong coupling confining regime has to be separated from the conformal phase, which corresponds to the range of gauge couplings attracted by the IR fixed point. Such kind of behavior has been documented, for example, for MWT or theories with a large number of fundamental flavors. Since we do not know *a priori* how far away our theory is from the conformal window, we have to consider the possibility of bulk transitions.

Bulk transitions have to be considered in a more general context. Pure $SU(2)$ Yang-Mills theory has a crossover from weak to strong couplings which becomes a bulk transition when an additional adjoint Wilson gauge action is coupled to the theory. Therefore, it is natural to expect bulk transitions for any theory with fermions in the adjoint representation. Moreover, there are a number of evidences for the bulk phases for theories with fermions in higher representation of the gauge group.

As first investigation, we monitor the expectation value of plaquette on small lattices as a function of β and κ . Similar studies have been done in earlier investigations in order to identify the bulk phase of MWT [35] and $SU(2)$ gauge theory with one adjoint Dirac flavor [17]. Note that these studies have been connected to the theory with a adjoint and fundamental plaquette action in [36]. In the



(a) Pure adjoint theory



(b) κ_F dependence

FIG. 1. The strong coupling phase transitions shown by discontinuity of the average plaquette as a function of the bare mass parameter. Figure 1(a) shows the pure adjoint theory ($\kappa_F = 0$). The transition can be observed for different lattice sizes of $N_s \times N_t = 4^4, 6^3 \times 8, 12^3 \times 16, 24^3 \times 48$. The dependence on mass of the fundamental fermions is shown in Fig. 1(b).

present case, the transition has to be mapped out in the space of β , κ_F , and κ_A . A scan of the parameter space is shown in Fig. 1. We have observed that the strongest transition appears in the pure adjoint case ($\kappa_F = 0$). The discontinuity gets weaker when the fundamental fermion part is added; see Fig. 1(b). In the present study, we want to connect our investigations to the pure adjoint and pure fundamental limit. Therefore, we have limited our main studies to the range of beta values above the transition in the pure adjoint case, $\beta \geq 2.1$. Despite the fact that only one Majorana fermion has been considered here and the fermion action is improved by the clover term, the results are quite consistent with the observations for MWT and $SU(2)$ gauge theory with one adjoint Dirac flavor, where a sharp transition appearing at around $\beta = 2.0$ has been observed [17,35]. It is important to note that the restrictions

appear to be weaker as soon as the fundamental fermions become dynamical.

IV. RELATION TO PURE $N_f = 2$ SU(2) FUNDAMENTAL

The SU(2) gauge theory with two fermions in the fundamental representation has been recently investigated in a series of publications; see [22–24] and references therein. As a first important step, we must cross-check our simulations by a comparison of our results with these studies. In these references, a different lattice action without clover improvement has been chosen. Therefore, a comparison in terms of physical units is required. In our studies, we measure in addition to the scale w_0 , the pseudoscalar (m_{PS}) and vector (m_V) meson masses. The corresponding operators are $\bar{\psi}_1\gamma_5\psi_2$ and $\bar{\psi}_1\gamma_k\psi_2$, respectively, where k denotes three different spacial directions. The same operators will be considered later also for the adjoint representation. In that case, the additional fermion field is considered in a partially quenched setup described in [37]. Note that the pseudoscalar meson is sometimes called pion (m_π) due to its similarities with the QCD pion state.

A. Scale setting and results in physical units

In the present studies, we use the parameter w_0 obtained from the gradient flow to fix the scale and for the conversion to physical units. The value of $\tau = w_0/a$ is defined from dependence of the action density E on the flow time τ as the point where the condition

$$\tau \frac{d}{d\tau} \tau^2 E(\tau) = W_{\text{ref}} \quad (2)$$

is fulfilled. The flow is taken from the Wilson gauge action and the clover antisymmetric definition is used for E on the lattice. We have chosen a reference scale of $W_{\text{ref}} = 0.3$ in most cases, which is the common value for scale setting in QCD. As shown in [38], large values of the reference scale are strongly influenced by the large autocorrelation times of topological quantities. Large- N_c analysis supports a scaling with N_c , which would lead to $W_{\text{ref}} = 0.2$ for SU(2) instead of $W_{\text{ref}} = 0.3$ for SU(3) [2]. Nevertheless, a reference scale of $W_{\text{ref}} = 1.0$ has been chosen in [24] and we have to consider this value for comparison in physical units. To mark the difference, we denote w_0/a the value at $W_{\text{ref}} = 0.3$ and \tilde{w}_0/a at $W_{\text{ref}} = 1.0$ in the following. The scales are linearly extrapolated as a function of $(am_{PS})^2$ to the chiral limit ($m_{PS} = 0$) to obtain $\tilde{w}_{0\chi}/a$ and $w_{0\chi}/a$. At $\beta = 2.1$, a linear fit in the range of $(am_{PS})^2 < 0.3$ yields a value of $\tilde{w}_{0\chi}/a = 4.17(9)$. Our limited data for $\beta = 2.2$ provide an estimate of $\tilde{w}_{0\chi}/a = 5.72(12)$.

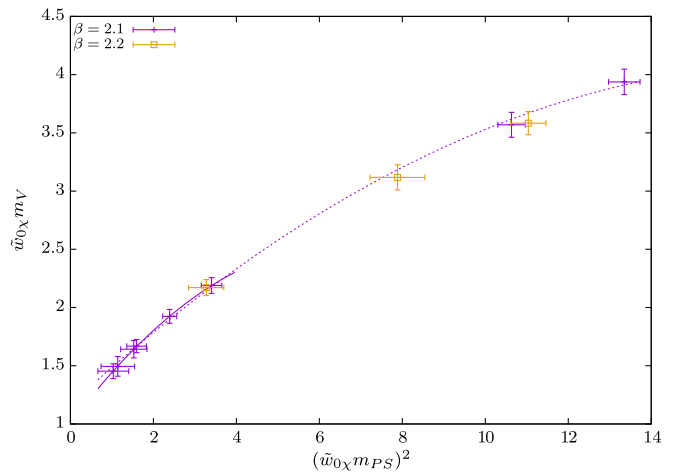


FIG. 2. The vector meson mass of the SU(2) $N_f = 2$ fundamental theory extrapolated to the chiral limit. A quadratic fit function is used for the $\beta = 2.1$ data. The dotted line indicates the fit of the complete range, but the final value is obtained only in the range $(w_{0\chi} m_{PS})^2 < 4$ indicated by the solid line. The $\beta = 2.2$ data are added for comparison.

B. The vector meson of clover improved pure fundamental runs

With the common scale setting, the physical value of the vector meson mass in the chiral limit can be compared to previous results for the SU(2) $N_f = 2$ pure fundamental theory. The extrapolation to the chiral limit is done including quadratic corrections as shown in Fig. 2. The fit of the complete range yields a value of $\tilde{w}_{0\chi} m_{V\chi} = 1.17(4)$. If we restrict the fit range, as done in [24], to $(\tilde{w}_{0\chi} m_{PS})^2 < 4$, the final result is $\tilde{w}_{0\chi} m_{V\chi} = 1.008(9)$, which is consistent with the continuum extrapolation of [24], $\tilde{w}_{0\chi} m_{V\chi} = 1.01(3)$. Note that comparing the same β value, the deviations from the continuum limit are smaller indicating an improvement by the clover term. The data at $\beta = 2.2$ are currently not sufficient to provide a fit in the relevant range, but it is compatible with the fit at $\beta = 2.1$. This also indicates that the results are close to the continuum.

Overall, there is a reasonable agreement between our study and earlier results in the pure fundamental case despite the absence of a continuum extrapolation. From the perspective of the pure fundamental theory, there seems to be no reason not to consider coarser lattices. The main limitation is due to the bulk phase induced by the adjoint fermions.

V. RELATION TO THE SU(2) ADJOINT LIMIT

The SU(2) pure adjoint limit corresponds to SYM theory. The simulations with one Majorana fermion require in this limit the RHMC algorithm and have a significantly higher computational cost than the pure fundamental limit. The validation of the results in this limit against our previous

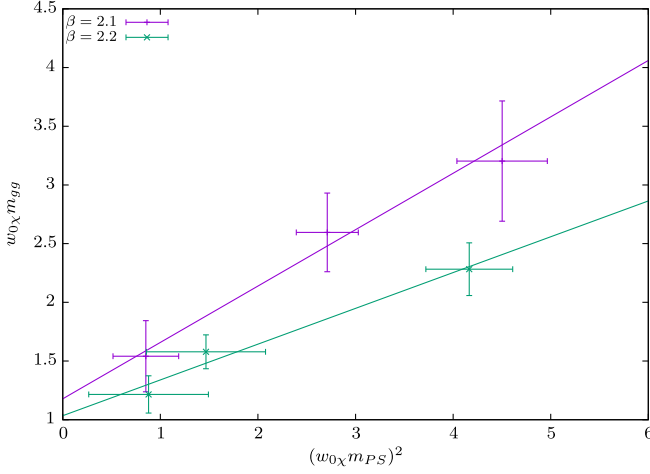


FIG. 3. The mass of the gluino-gluon particle in the pure adjoint limit (supersymmetric Yang-Mills theory). The plot shows a linear chiral extrapolation in units of $w_{0\chi}$ as a function of the square of the adjoint pion mass m_{PS} .

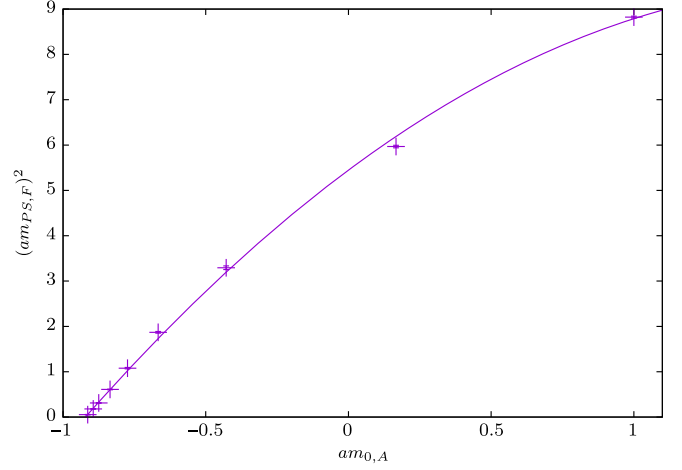
data is required since the simulation setup and the lattice action have been changed.

There are no simple physical mesonic states without disconnected contributions in this theory. The adjoint pion mass, corresponding to m_{PS} , determines the deviations from the chiral limit using partially quenched chiral perturbation theory [37]. All particles require rather involved measurements with large statistics, which is inaccessible in this study. The only estimate of a bound state that we can access is the mass of the fermionic gluino-gluon particle defined by the operator $\sum_{\mu,\nu} \sigma_{\mu\nu} \text{Tr}[F^{\mu\nu}\lambda]$; see [39] for further details. This can be compared to our previous results in units of $w_{0\chi}$.

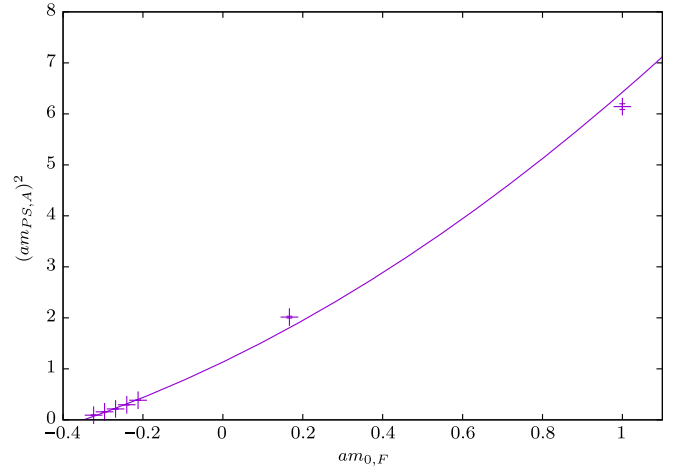
We have generated only a small number of runs, and consequently the fit range is insufficient for a precise chiral extrapolation. The rough estimates based on a linear fit are $w_{0\chi}/a = 2.42(22)$ at $\beta = 2.1$ and around $w_{0\chi}/a = 3.85(9)$ at $\beta = 2.2$. More precise data would require to consider a larger range of masses since higher order corrections might be relevant. The gluino-gluon mass in units of the scale $w_{0\chi}$ can be extrapolated to the chiral limit, as shown in Fig. 3. We obtain a value of $w_{0\chi} m_{gg} = 1.18(18)$ at $\beta = 2.1$ and $w_{0\chi} m_{gg} = 1.03(14)$ which is close enough to our previous continuum extrapolation $w_{0\chi} m_{gg} = 0.93(6)$ in [39].

VI. SCENARIOS FOR THE MIXED FUNDAMENTAL-ADJOINT THEORY

In the previous sections, we have confirmed the reliability of our simulations in the limiting pure fundamental and pure adjoint cases. The current first study of the mixed representation theory is organized in such a way that both limiting cases can be reached with the same bare coupling. This means that the range of β is limited by the pure adjoint



(a) Dependence on adjoint bare mass



(b) Dependence on fundamental bare mass

FIG. 4. Dependence of the pseudoscalar mass in one representation on the bare mass parameter of the other. In Fig. 4(a), κ_F is fixed to 0.1350 and in Fig. 4(b) κ_A is fixed to 0.1600. The quadratic fit is added to illustrate the qualitative trend.

bulk transition. In later studies, even smaller β might be considered since the transition is weakened by the fundamental fermions.

A possible scenario for the theory is a spontaneous chiral symmetry breaking in the limit where both masses tend to zero (chiral limit). Like in QCD, Goldstone bosons are expected to interact accordingly to chiral perturbation theory in the small mass regime. Alternatively, this theory could be close to an infrared conformal fixed point (IRFP). Near an IRFP, the masses of all particles scale to zero with an exponent provided by the mass anomalous dimension. In a walking or near conformal regime, the behavior could be quite similar, even though it is difficult to quantify the distance to the conformal case. Hence, it could be that the theory shows already signs of conformality even if a chiral symmetry breaking scenario is obtained in the deep infrared.

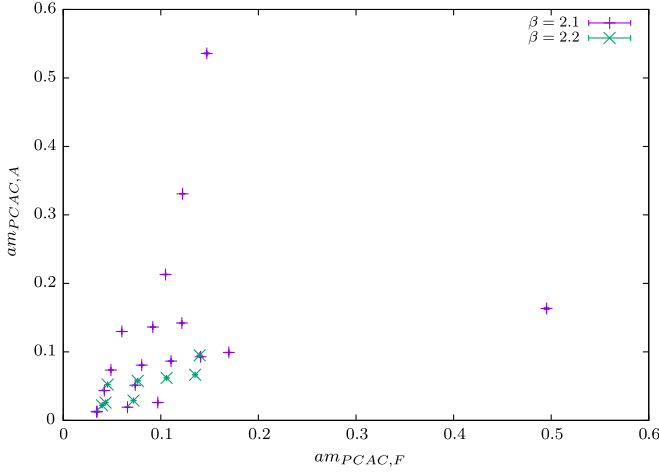


FIG. 5. Range of masses obtained from the partially conserved axial current (PCAC) relation for both of the representations. The adjoint PCAC mass $m_{PCAC,A}$ and one of the fundamental representations $m_{PCAC,F}$ are shown in lattice units for the two different values of the coupling β .

In the following, we investigate to what extends these two scenarios are reflected in the numerical data. The fact that two different fermion representations are considered leads to some complications, for instance, related to the parameter tuning and scale setting, that will be explained in the following.

A. Parameter tuning and scale setting

The tuning of the bare mass in one representation shows a clear dependence on the mass parameter of the other, as illustrated in Fig. 4. Such a dependence complicates the tuning of the theory toward the chiral limit. Note, however, that the bare parameter dependence is not the relevant quantity for fits of chiral perturbation theory in case of Wilson fermions. The mass for the chiral fits is obtained from the partially conserved axial current (PCAC) relation (m_{PCAC}). The PCAC masses in both representations for the relevant simulations are shown in Fig. 5.

Another observation is a significant increase of the flow scale. At $\beta = 2.1$, $\kappa_F = 0.1360$, $\kappa_A = 0.1620$, the value of $w_0/a = 4.639(77)$ is obtained, which is significantly larger than values at a similar $m_{PS,A}$ in the pure adjoint case (between $w_0/a = 2.289(11)$ and $3.348(22)$ at the same β). This indicates a slow running of the coupling. In addition, the topological fluctuations are suppressed, which in turn leads to a large autocorrelation of w_0/a . Due to this reason and the small statistic, the values for this quantity at $\beta = 2.2$ are currently not reliable. A very rough estimate of can be obtained in a chiral extrapolation as a function of the adjoint PCAC mass, which is the dominant dependence compared to the PCAC mass of the fundamental representation. This leads to a prediction of $w_0/a = 4.9(2)$ at $\beta = 2.1$. The data at $\beta = 2.2$ are within very large errors

consistent with this value, but they show a strong correlation with the topological charge. Note that all of our runs are based on a minimum of 300 thermalized configurations. Further discussions of the problem of topological freezing and estimates of induced systematic uncertainties can be found in Appendix A.

VII. CHIRAL PERTURBATION THEORY AND CHIRAL EXTRAPOLATIONS

Chiral perturbation theory with two different representations has been worked out in [1] and applied in the analysis of lattice data in [2]. As a first step, it is already instructive to test the approximation that neglects the interdependence of the two fermion species. This means to apply a fit function according to $N_f = 2$ chiral perturbation theory for the fundamental representation. The breaking pattern for the gauge group $SU(2)$ is [22]

$$SU(2N_f^{(F)}) \rightarrow Sp(2N_f^{(F)}), \quad (3)$$

leading to three pseudoscalar and two scalar Goldstone states. The breaking pattern for the adjoint representation is

$$SU(2N_f^{(A)}) \rightarrow SO(2N_f^{(A)}). \quad (4)$$

For one adjoint Majorana fermion, an approach based on partially quenched chiral perturbation theory has to be used, in which the disconnected part of the pseudoscalar meson (adjoint pion) becomes massless in the chiral limit [37]. A PCAC mass is measured from the disconnected correlators, which is the same measurement as for $N_f^{(A)} = 1$, but with gauge configurations of the $N_f^{(A)} = 1/2$ theory.

We consider first a fit of $(m_{PS})^2$, which is linear in m_{PCAC} at leading order, including also quadratic corrections; see Fig. 6. Here and in the following considerations, the fits are related only to the data at $\beta = 2.1$. A complete summary of the data can be found in Appendixes B and C. At small m_{PCAC} , the fit captures the main dependence, but for the fundamental representation there are considerable differences at larger $m_{PCAC,F}$. This already indicates corrections at the order of the product of the two masses. These corrections seem to be much smaller for the adjoint representation.

In order to include the corrections from the mutual interactions of the fields in the other representation, the fit must include two dimensions. Due to our currently limited data, we consider only the leading contributions in [2]. Higher order terms are either of logarithmic form or describe lattice artifacts and a determination of the coefficients would require more data and different lattice spacings. In the expected functional dependence,

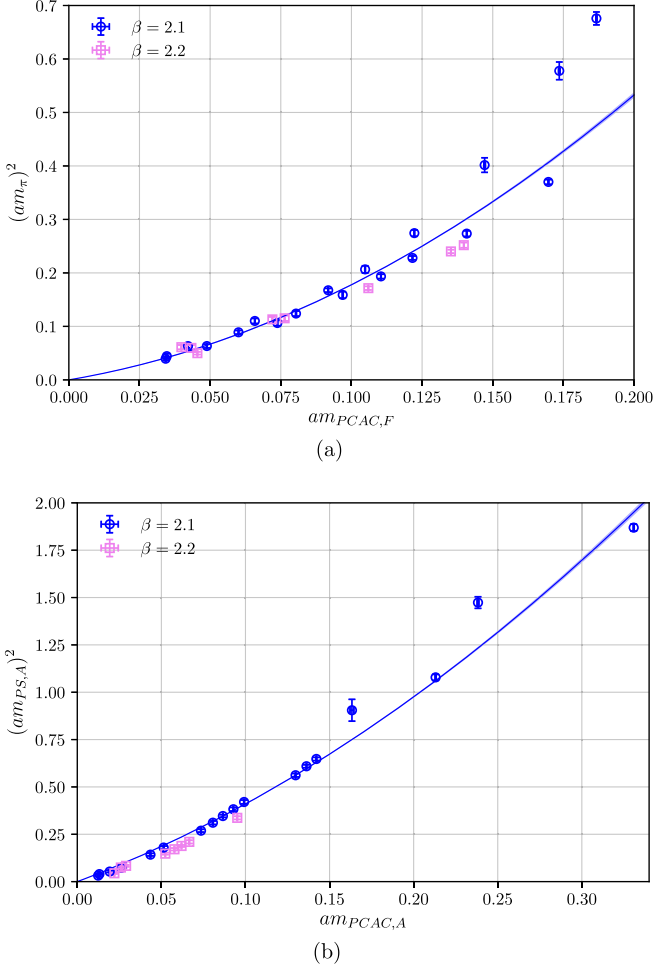


FIG. 6. Dependence of the pseudoscalar mass on the PCAC mass of the same representation. (a) shows the fundamental and (b) the adjoint case. The leading order of chiral perturbation theory predicts a linear behavior of m_{PS}^2 . The fit includes an additional quadratic correction, but not the dependence on the mass of the other representation.

$$(am_{\text{PS},F})^2 = c_1 am_{\text{PCAC},F} + c_2 am_{\text{PCAC},F} am_{\text{PCAC},A} + c_3 (am_{\text{PCAC},F})^2 \quad (5)$$

$$(am_{\text{PS},A})^2 = c_1 am_{\text{PCAC},A} + c_2 am_{\text{PCAC},F} am_{\text{PCAC},A} + c_3 (am_{\text{PCAC},A})^2, \quad (6)$$

the unknown parameters c_1 , c_2 , and c_3 need to be determined by the fit. In order to handle finite size effects, we have excluded $m_{\text{PS}}L < 7$ for both representations. We have tested several different cuts for the fit ranges to optimize the goodness of fit ($\chi^2/\text{d.o.f}$). The final fitting intervals include 11 and 10 points and are restricted to $am_{\text{PCAC},F} < 0.2$, $am_{\text{PCAC},A} < 0.6$ for $(am_{\text{PS},F})^2$, and $am_{\text{PCAC},F} < 0.5$, $am_{\text{PCAC},A} < 0.3$ for $(am_{\text{PS},A})^2$.

The fitted parameters are summarized in Table I. The results show that the dominant contribution comes from the

TABLE I. Summary of the fit results for the pion masses. The fit range has been restricted to $am_{\text{PCAC},F} < 0.2$; $am_{\text{PCAC},A} < 0.6$ for $(am_{\text{PS},F})^2$ and $am_{\text{PCAC},F} < 0.5$; $am_{\text{PCAC},A} < 0.3$ for $(am_{\text{PS},A})^2$. The last column specifies the reduced chi-square. Note that the reduced chi-square without the mass of the second representation (c_2) was a factor of 7 (for $m_{\text{PS},F}$) and 4 (for $m_{\text{PS},A}$) larger.

	c_1	c_2	c_3	$\chi^2/\text{d.o.f}$
$(am_{\text{PS},F})^2$	0.902(22)	1.725(82)	6.40(18)	8
$(am_{\text{PS},A})^2$	2.941(80)	2.11(51)	9.47(50)	0.8

mass of the same representation with still a significant mixing with the other representation.

Apart from m_{PS} , the chiral symmetry breaking scenario can also be checked with the pseudoscalar decay constant f_{PS} . The dependence on the fermion mass in the same representation is shown in Fig. 7. In case of the

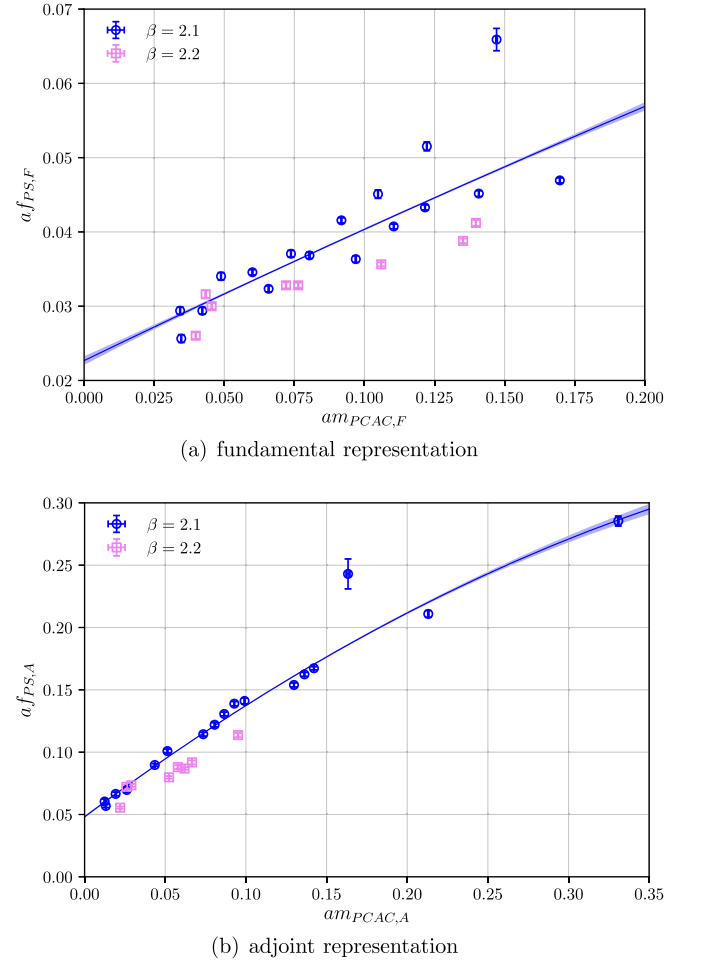


FIG. 7. Dependence of the pseudoscalar decay constant on the PCAC mass of the same representation. (a) shows the fundamental and (b) the adjoint case. Compared to the functions (7) and (8), the fit includes an additional quadratic correction, but not the dependence on the mass of the other representation. The fit in Fig. 7(b) is considered in the range $am_{\text{PCAC},A} < 0.11$.

TABLE II. Summary of the fit results for the pseudoscalar decay constants. The fit ranges are the same as in Table I. Note that the reduced chi-square without the mass of the second representation (c_2) is a factor of 5 (for $f_{\text{PS},F}$) and 6 (for $f_{\text{PS},A}$) larger.

	c_0	c_1	c_2	$\chi^2/\text{d.o.f}$
$af_{\text{PS},F}$	0.02465(46)	0.1139(37)	0.0387(19)	11
$af_{\text{PS},A}$	0.0591(22)	0.668(15)	0.116(16)	1.4

fundamental representation, it indicates clearly an additional dependence on the adjoint mass. We are again only able to extract the leading behavior of the dependence [2],

$$af_{\text{PS},F} = c_0 + c_1 am_{\text{PCAC},F} + c_2 am_{\text{PCAC},A}, \quad (7)$$

$$af_{\text{PS},A} = c_0 + c_1 am_{\text{PCAC},A} + c_2 am_{\text{PCAC},F}. \quad (8)$$

This fit resolves the dependence on the two masses, as can be seen in Table II. Note that there is still a rather large residual for the fundamental representation, which could be due to higher order corrections but also to the current limited precision of the data.

Besides the expected massless states in the scenario of chiral perturbation theory, we can also look at the vector states m_V . In case of the adjoint representation, this is again not a physical particle of the theory, but it is obtained in the partially quenched setup considering only the disconnected part of the correlator. It is extrapolated to a constant value in the chiral limit and we consider linear and quadratic corrections in the fit. As shown in Fig. 8, there are again considerable deviations in case of the fundamental representation, whereas for the adjoint representation the dependence in $m_{\text{PCAC},A}$ seems to be dominant. The mass of the gluino-gluon particle m_{gg} can also be extrapolated to the chiral limit as a function of $m_{\text{PCAC},A}$, but due to the limited statistics there are much larger uncertainties and the errors are currently underestimated, see Fig. 9(a) and similar for w_0/a Fig. 9(b).

A generic fit ansatz for m_V (and m_{gg}) are the following functions:

$$am_{V,F} = c_0 + c_1 am_{\text{PCAC},F} + c_2 am_{\text{PCAC},A}, \quad (9)$$

$$am_{V,A} = c_0 + c_1 am_{\text{PCAC},A} + c_2 am_{\text{PCAC},F}, \quad (10)$$

$$am_{gg} = c_0 + c_1 am_{\text{PCAC},A} + c_2 am_{\text{PCAC},F}. \quad (11)$$

We have tested higher order corrections, but it turned out that they are not significant and cannot be reliably estimated in this case. We have considered the same fit ranges as for m_{PS} . The results are summarized in Table III. The dominant contribution comes still from the fermion mass in the same representation. In case of the adjoint

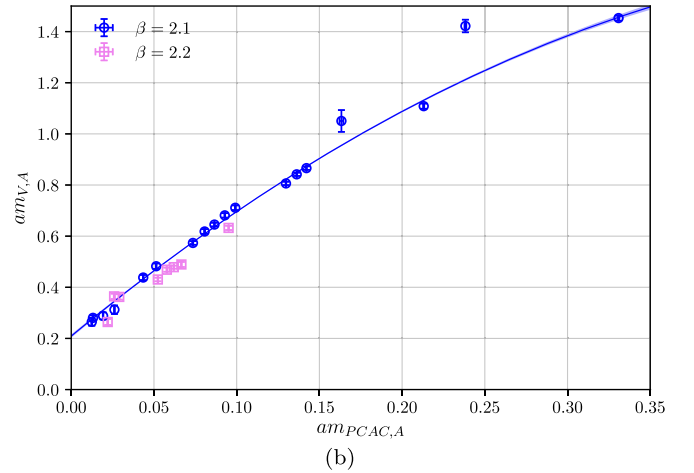
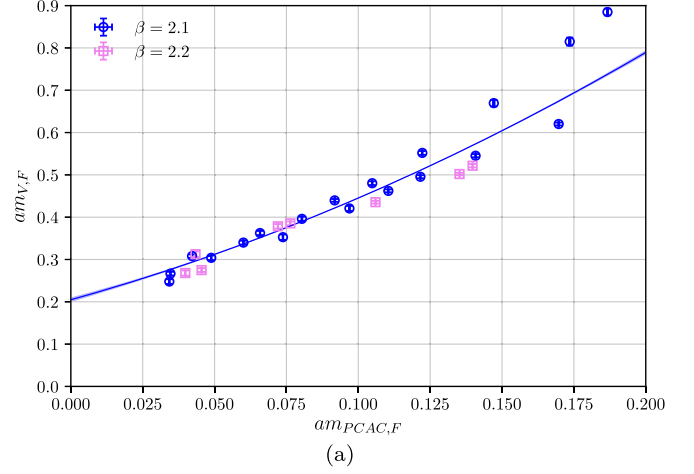
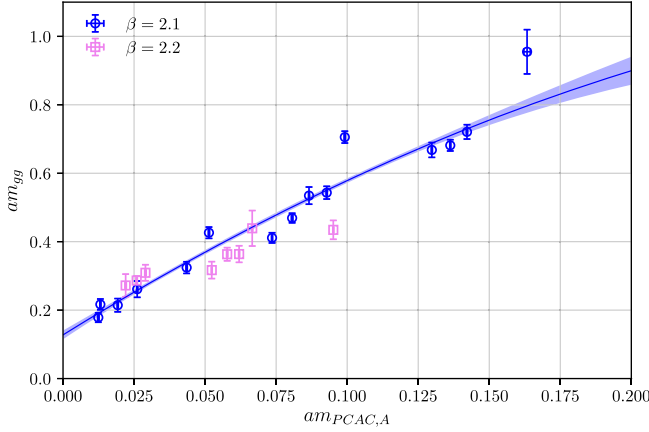


FIG. 8. Dependence of the vector meson mass on the PCAC mass of the same representation. (a) shows the fundamental and (b) the adjoint case. The fit is done with a constant and up to quadratic corrections ignoring the dependence on the mass of the other representation.

representation, it is not even clear that the inclusion of the mass of the fundamental representation provides a more reliable fit. The gluino-gluon mass is clearly dominated by the fermion mass of the adjoint representation and the inclusion of the fundamental representation seems not necessary given the current uncertainties.

TABLE III. Summary of the fit results for the pion masses. The last two columns specify the fit ranges and reduced chi-square. Note that the reduced chi-square without the second representation (c_2), but including instead a quadratic correction, is a factor of 10 larger for $m_{V,F}$. For $m_{V,A}$, the reduced chi-square is approximately the same and for m_{gg} it is larger by a factor of 2.

	c_0	c_1	c_2	$\chi^2/\text{d.o.f}$
$am_{V,F}$	0.1625(50)	2.545(40)	0.241(13)	4
$am_{V,A}$	0.288(11)	3.825(70)	0.258(67)	2
am_{gg}	0.213(20)	2.82(16)	0.80(13)	6



(a) Gluino-gluon mass

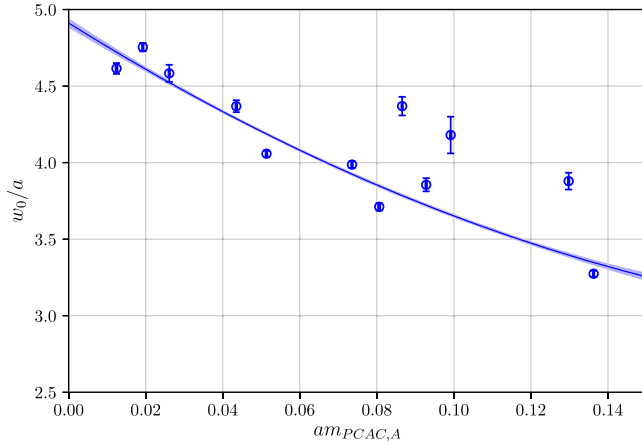
(b) w_0/a chiral extrapolation

FIG. 9. Chiral extrapolations of the gluino-gluon mass (a) and the scale w_0/a (b) as a function of the adjoint PCAC mass, neglecting the dependence on the fundamental mass. Only the data for $\beta = 2.1$ are shown in Fig. 9(b).

The range of m_V and m_{PS} in our simulations requires some further comments when compared to simulations of QCD. Usually a small m_{PS}/m_V value would be preferred for chiral fits. However, in a conformal theory, these ratios are close to $m_{PS}/m_V \approx 1$. The theory considered here is quite close to the conformal case and it is consequently difficult to reach a regime of $m_{PS}/m_V \ll 1$.

The figures have been presented in lattice units to show the general functional dependence and avoid additional errors from the scale setting. In Fig. 10, m_V is represented in physical units to allow for a better comparison of the general scale. Note, however, that the scale setting quantities w_0 and f_{PS} are affected by the topological freezing which leads to additional systematic uncertainties. Another representation in physical units is provided by the mass ratios; see Fig. 12.

In addition, we want to comment further on the relevance of higher order corrections in view of a larger reduced chi-square for $am_{PS,F}$ and $af_{PS,F}$ in Tables I and II. We have

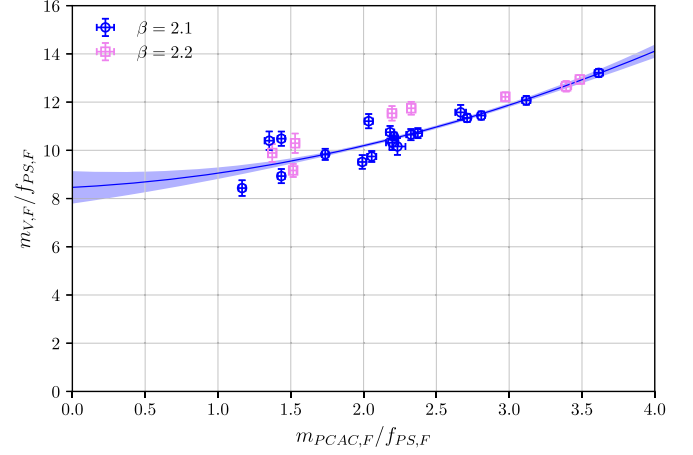


FIG. 10. Dependence of the vector meson mass on the PCAC mass of the same representation as in Fig. 8(a). This plot represents the values in units of $f_{PS,F}$.

tested a fit of $am_{PS,F}$ with higher order corrections including a logarithmic term and a term linear in $am_{PCAC,A}$, but it leads only to an increase of the reduced chi-square. In case of $af_{PS,F}$, these corrections lead to a slightly smaller reduced chi-square (approximately 9), but a negative c_1 is preferred, which renders this fit unreasonable. We therefore conclude that more data are needed to constrain the additional parameters.

We have also done a number of simulations at a larger value of β equal to 2.2. In Figs. 6, 7, and 9(a), we have added these data to the fit at $\beta = 2.1$. Compared to the other uncertainties, only a rather small dependence on the gauge coupling can be observed. From the present data, we are not able to resolve a continuum extrapolation.

VIII. CONFORMAL SCENARIO

In a conformal scenario, the behavior of the theory is influenced by an infrared fixed point (IRFP) of the massless theory. If the scalar matter fields and their interactions were included in the Lagrangian of our theory, the corresponding SQCD theory has $N_c = 2$, $N_f = 2$ and is conjectured to be outside the conformal window [40]. Naively, the scalar matter fields are expected to decrease the running of the coupling (β -function) and bring the evolution toward an IRFP. Hence, the conformal scenario is not expected in our theory with $N_f^{(F)} = 2$ and $N_f^{(A)} = 1/2$. Nevertheless, it is interesting to check for a walking (near conformal) scenario, which has been conjectured for the theory with $N_f^{(A)} = 1$ based on perturbative estimates. In such a scenario, it is assumed that in a certain range of scales the β -function is already strongly influenced by an IRFP appearing at a larger N_f . In this range of scales, it should be close to a conformal scenario. We therefore test the scaling of the masses to the chiral point assuming the presence of an IRFP. More generally, the difference between a chirally

broken or a conformal scenario is quite subtle for theories close to the lower edge of the conformal window, and we also want to investigate how well the two scenarios can be distinguished.

In the conformal case, the masses are relevant directions of the renormalization group transformation in the vicinity of the IRFP, while the gauge coupling is irrelevant. If one considers N_f fermions in one single representation, each mass is an independent relevant direction. However, they all have a common scaling dimension and it is therefore rather trivial to consider the RG flow in the manifold spanned by the mass parameters. The theory defined by a certain RG trajectory is determined by the ratios of the different mass parameters. In a simplified setup, one can consider just two relevant directions defined by the mass of $(N_f)_h$ heavy and $(N_f)_l$ light flavors. The flow is in this case defined by the ratio of the two masses. The mass parameters can be used to tune the running of the gauge coupling to a walking scenario. Projected onto the plane of the gauge coupling, the two mass parameters introduce an intermediate region of scales with a small running of the gauge coupling. This is the basic idea of the scenario proposed in [26,27].

The situation becomes more complicated for a theory with two different representations, since the anomalous dimensions of the two relevant mass parameters are not the same. We therefore recall some of the arguments presented in [26,27,41] and extend them to the current case. When the scale is changed by $\mu \rightarrow \mu/b$ ($b > 1$), the scaling of a correlation function near the fixed point is given by

$$C_H(t, g_i, m_i, \mu) = b^{-2y_H} C_H(t/b, b^{y_{g_i}} g_i, b^{y_i} m_i, \mu/b), \quad (12)$$

with scaling exponents of the operator y_H and the relevant mass directions with scaling dimension y_i . The irrelevant couplings g_i with scaling dimension $y_{g_i} < 1$ can be approximately set to their fixed point value and are ignored in the following. We can assume that the scale is set by one of the mass parameters $b = m_1^{-1/y_1}$, while the other fermions are below the decoupling scale ($m_1^{-y_i/y_1} m_i$ is small enough). The scaling is simplified to ($i \neq 1$)

$$C_H(t, m_1, m_i) = m^{-2y_H/y_1} C_H(t m_1^{1/y_1}, m_i / (m_1^{y_i/y_1})). \quad (13)$$

For large t , the correlation function approaches the exponential form $\exp(-M_H t)$ with the mass of some state M_H . Consequently, all particle masses should scale like m_1^{1/y_1} and the dependence on other mass parameters is via the ratio $m_i m_1^{-y_i/y_1}$, or equivalently $m_1 m_i^{-y_1/y_i}$. As shown in [27], mass ratios can be considered to cancel the leading m_1^{1/y_1} dependence.

In our case, we can consider the ratio of vector and pseudoscalar mesons, for example, in order to check

whether it can be represented by a functional dependence F_R given by

$$\frac{am_{V,F}}{am_{PS,F}} = F_R(am_{PCAC,F}(am_{PCAC,A})^{-y_F/y_A}). \quad (14)$$

This study requires the determination of anomalous dimensions γ_F and γ_A for adjoint and fundamental representation, which define the scaling $y_i = 1 + \gamma_i$.

For this reason, let us first investigate the leading dependence $M_H \sim m_i^{1/(1+\gamma_i)}$. Therefore, we consider for each state only the leading dependence, either $m_1 = m_f$ or $m_2 = m_a$, already determined in the chiral fits of Sec. VII. The simplest way to extract the leading exponents is a linear fit in a double logarithmic representation. We have done this using $am_{PS,F}$ and $am_{V,F}$ as a function of $am_{PCAC,F}$ [Fig. 11(a)]. A fit of the mass $am_{PS,F}$ leads to

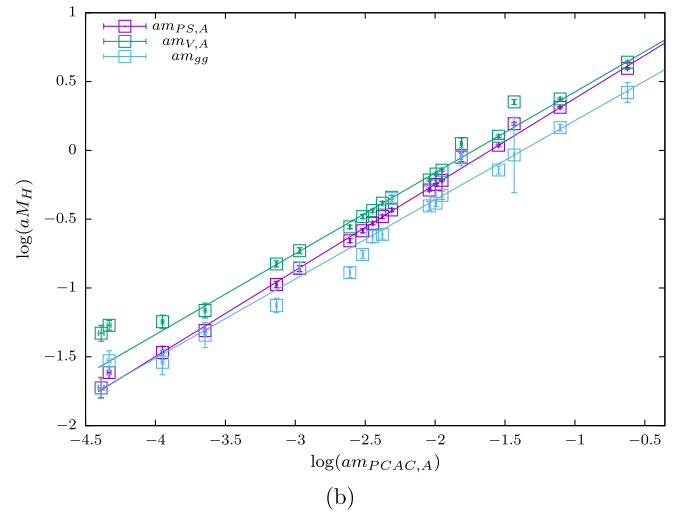
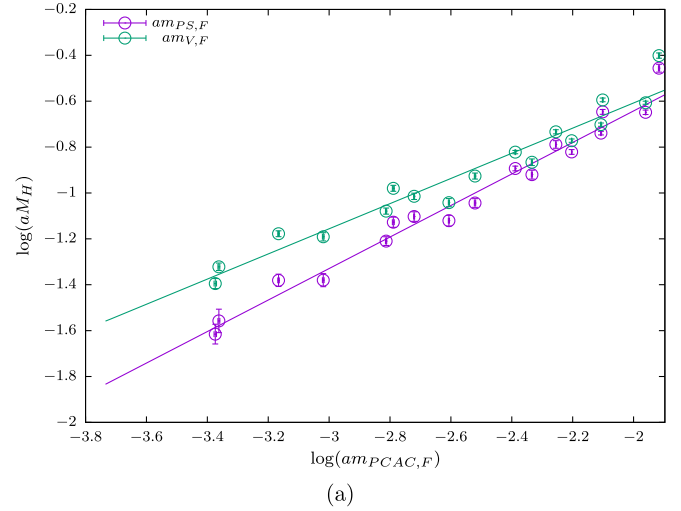


FIG. 11. Double log representation of the dominant dependence of the bound state masses on the two mass parameters. (a) shows the fundamental and (b) the adjoint case. The linear fit assumes an approximate scaling near an IRFP.

TABLE IV. Summary of the approximate leading scaling dimensions obtained with the fits in logarithmic representation, Fig. 11.

$am_{\text{PS},F}$:	$y_F = 1.46(8)$	$am_{V,F}$:	$y_F = 1.82(30)$
$am_{\text{PS},A}$:	$y_A = 1.60(2)$	$am_{V,A}$:	$y_A = 1.70(4)$
am_{gg} :	$y_A = 1.26(12)$		

a scaling dimension $y_F = 1.46(8)$. According to the assumed conformal behavior, $am_{V,F}$ is expected to show approximately the same scaling, but a considerable deviation is observed which might be due to the additional dependence on $am_{\text{PCAC},A}$. This is also reflected by the large error of the obtained scaling dimension. The fit of $am_{\text{PS},A}$, $am_{V,A}$, and am_{gg} shows a quite consistent scaling as a function of $am_{\text{PCAC},A}$ [Fig. 11(b)]. All obtained scaling dimension are listed in Table IV. Overall, the fits indicate a slightly larger y_A , but the ratio $r = y_F/y_A$ is still above 0.5. We have also used the mode number with the same methods as in [18] to estimate the mass anomalous dimension for the run with the smallest masses for both representations. Since we have not done a careful analysis of the mass dependence, only a rough estimate can be provided from this method, which is $\gamma_F \approx 0.3$ and $\gamma_A \approx 1.0$. In summary, these investigations of the leading dependence indicate a γ_F in the range 0.3–0.5 and γ_A in the range 0.3–1.0, assuming conformal scaling. This implies that $r = y_F/y_A$ is expected to be at least above 0.3.

The leading scaling can be used to investigate finally the subleading dependence (14). We have investigated the ratio of $m_{V,F}/m_{\text{PS},F}$ as a function of $am_{\text{PCAC},F}(am_{\text{PCAC},A})^{-r}$. The fit according to $a + b/(am_{\text{PCAC},F}(am_{\text{PCAC},A})^{-r})$ can be used to optimize the residual as a function of r . In this process, we observe that small values of $r < 0.4$ are

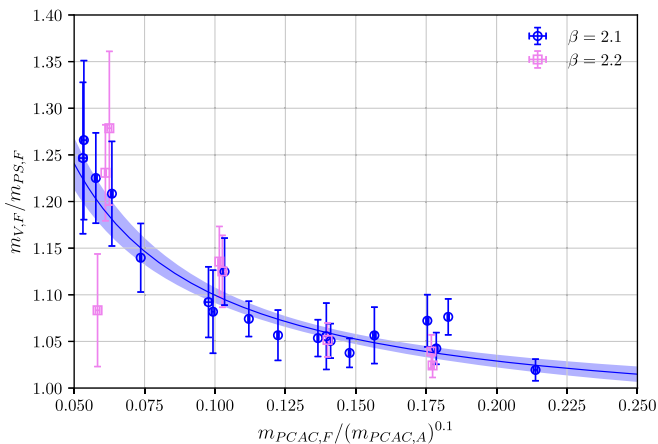


FIG. 12. The ratio of vector over pseudoscalar mass in the fundamental representation as a function of $am_{\text{PCAC},F}(am_{\text{PCAC},A})^{-r}$. The line shows a fit according to $a + b/x$ of the $\beta = 2.1$ data. The value of $r = 0.1$ corresponds to an optimal choice according to the residual.

preferred and a value of $r = 0$ cannot be excluded, see Fig. 12, indicating rather a chiral symmetry breaking than a conformal scenario. The best fit is obtained with $r = 0.1$, which is clearly outside the region predicted by conformal scaling. Note, however, that the ratio $m_{V,F}/m_{\text{PS},F}$ still shows only a weak dependence on the masses and the consistent scaling in Fig. 12 leads to almost constant ratios between the masses in this figure.

IX. CONCLUSIONS

We have presented the first results of the simulations with a gauge theory coupled to fermions in adjoint and fundamental representation. The present work provides a preparatory study for further simulations of SQCD, UMWT, or compactified SYM with fundamental matter. In the current study, we have considered SU(2) gauge theory with one Majorana fermion in the adjoint representation and two fundamental flavors. This corresponds to two flavor SU(2) SQCD without scalar fields.

We have presented cross-checks with existing results in the pure adjoint and fundamental limit. In a first investigations we have also determined the reliable range of parameters by an investigation of the bulk transition.

The main objective of this work has been the determination of signals for a chiral symmetry breaking or a conformal scenario since the realization of these distinct infrared scenarios will affect any further investigation of the theory. We have derived scaling relations for theories with two different fermion representation according to an IR conformal scenario. We have compared our numerical data to the expected functional dependence in the conformal and the chiral symmetry breaking case. In the conformal case, we have found no consistent scaling determined by scaling dimensions y_F and y_A .

Our investigation shows that the theory is consistent with a chiral symmetry breaking scenario, but still close to the conformal window. The running of the gauge coupling is quite small and mass ratios are nearly constant. This situation is similar to what is expected for SU(2) SQCD with two flavors, since the conformal window is predicted to start close by at $N_f = \frac{3N_c}{2}$. The number of colors N_c would have to be increased in order to get a more significant difference from the conformal case with two flavor SU(N_c) SQCD.

The bare parameter tuning with Wilson fermions of one representation seems to be considerably affected by the other. The dependence on physical mass parameters is provided by the two PCAC masses. We observe a rather mild dependence of the states in one representation on the mass of the other. The most significant effect has the adjoint fermion mass since the fundamental meson masses clearly depend on it. Furthermore, the adjoint mesons and the gluino-gluon can be extrapolated to the chiral limit considering as a good approximation only the dependence on the adjoint mass.

Regarding the simulations of SU(2) two flavor SQCD, the following strategy could be derived from the data. Since the system is close to the conformal window, one might neglect the running of marginal couplings like the gauge coupling and set them to their tree level value. The important extrapolation of the pure SYM part to the chiral limit can be done as a first approximation just from the adjoint PCAC mass, which might capture the leading dependence. Note, however, that due to Yukawa couplings the chiral transformations of fundamental and adjoint fermions are not independent in SQCD. The Yukawa terms are only invariant under a combined transformation of the two fermion fields and the scalar field.

In order to investigate in more detail, the conformal scenario with two different representations, a larger number of adjoint fields should be considered. One interesting investigation is the simulation of UMWT, which means one Dirac instead of one Majorana fermion in the adjoint representation.

The current data correspond to a first investigation of the theory. A larger statistic, a more complete scan of the relevant parameter range, and a more careful considerations of methods such as the mode number measurement for two fermion representations would be required to provide more precise data. Note, however, that the parameter scan with two independent fermion representations will require a considerably larger amount of computational resources.

The choice of the parameters provides particular challenges in the current close to conformal theory with two representations. In principle, one would like to avoid bulk phases for the complete range of mass parameters, which is achieved by a sufficiently large β . Due to strong influence of the fermions on the running of the gauge coupling, this leads, however, to large finite size effects and topological freezing when both fermion masses become small. One way to avoid this is to adjust the gauge coupling depending on the fermion masses, but this might lead to a more difficult scale determination and possible remnant effects of bulk phases.

ACKNOWLEDGMENTS

The authors gratefully acknowledge the Gauss Centre for Supercomputing e.V. [42] for funding this project by providing computing time on the GCS Supercomputer SuperMUC at Leibniz Supercomputing Centre [43]. Further computing time has been provided on the compute cluster PALMA of the University of Münster. G.B. acknowledges support from the Deutsche Forschungsgemeinschaft Grant No. BE 5942/2-1.

APPENDIX A: TOPOLOGICAL CHARGE FLUCTUATIONS

An important issue for the simulation is a freezing of the topological charge leading to simulations at an

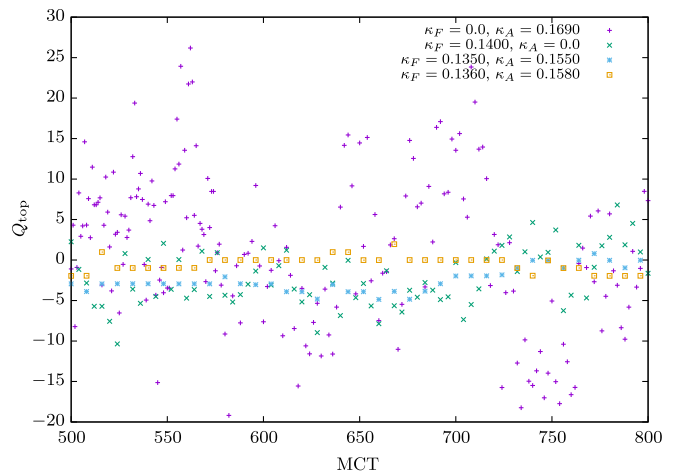


FIG. 13. Subset of the Monte Carlo history for the topological charge determined from the gradient flow. Runs for different mass parameters on a $24^3 \times 48$ lattice at $\beta = 2.1$ are compared.

effectively fixed topology. It is known that this effect sets in for QCD simulations at fine lattices and large β . We observe also a strong dependence on the fermion masses. This is illustrated in Fig. 13. In the pure adjoint and pure fundamental cases, the fluctuations of the topological charge are quite considerable, while toward the chiral limit of the two representations, topology gets almost frozen.

The method used to measure the topological charge and the effect of topological freezing on w_0 is explained in [38]. In this reference, it is also shown that the systematic uncertainty increases at larger β . The effect is hard to determine from the autocorrelation time of our current rather short runs. In order to estimate the systematic effect, we have separated for the run at $\beta = 2.1$, $\kappa_A = 0.1580$, $\kappa_F = 0.1360$ the configurations according to topological sectors $Q_{\text{top}} = -1$ and $Q_{\text{top}} = 0$. A rough estimate for the uncertainty is provided by the difference of averages between the two sectors. Most observables do not show a significant deviation apart from af_{PS} (approximate difference 0.006) and w_0/a (approximate difference 0.3). Assuming that all runs are affected in a similar way by a fixed topology, this provides an estimate for the additional systematic uncertainty. In Fig. 14, we illustrate the relevance of this effect for the observables. In this figure, we have also added the $\beta = 2.2$ data for comparison. As expected, the extrapolation of w_0/a gets larger errors and the scattering of the $\beta = 2.2$ data shows that the effect becomes even more severe at larger β . On the other hand, af_{PS} shows a smaller scattering of the data at the larger β and it could be that the systematic error is therefore actually smaller than our estimate.

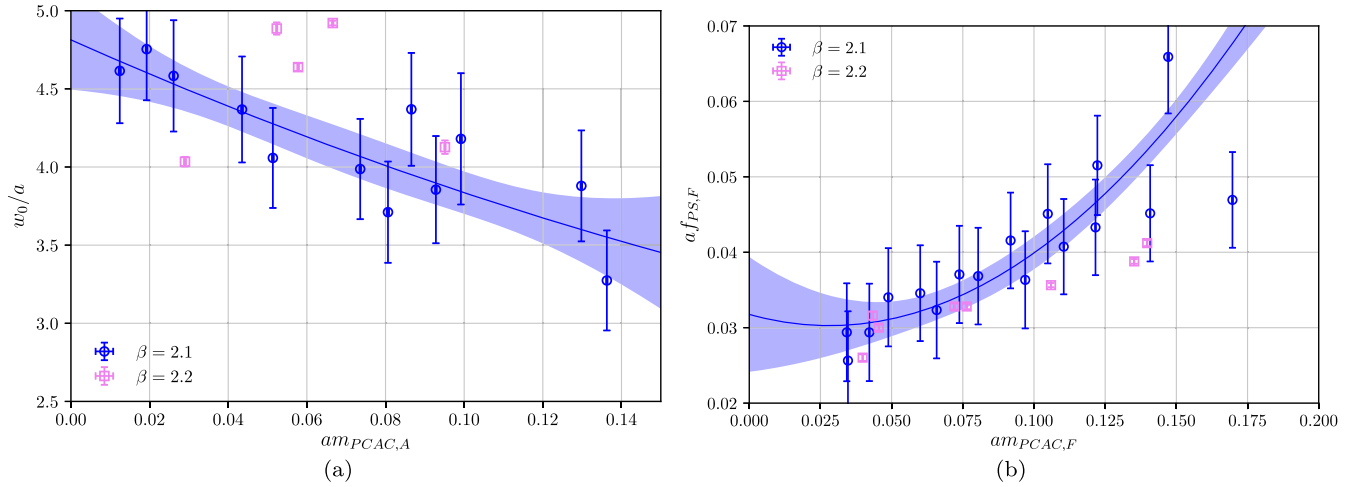


FIG. 14. The same data as in Figs. 7(a) and 9(b) with an additional estimate of the systematic error due to the frozen topology. As a rough approximation, the same additional systematic error is assumed at all points. In case of w_0/a also, the $\beta = 2.2$ data have been added for comparison. (a) shows the chiral extrapolation for w_0/a and (b) for $af_{PS,F}$.

APPENDIX B: SUMMARY OF THE DATA: PURE ADJOINT AND PURE FUNDAMENTAL RUNS

β	$N_s \times N_t$	κ_F	$am_{PS,F}$	$am_{V,F}$	w_1/a	N_{conf}
2.1	24×48	0.1350	0.8762(69)	0.9443(58)	2.3953(50)	587
2.1	24×48	0.1360	0.7819(63)	0.8559(71)	2.5433(64)	502
2.1	24×48	0.1390	0.4423(61)	0.5249(49)	3.287(12)	800
2.1	24×48	0.1395	0.3709(42)	0.4614(43)	3.426(12)	2600
2.1	24×48	0.1400	0.2964(87)	0.3937(93)	3.753(30)	684
2.1	24×48	0.1403	0.256(11)	0.358(12)	3.878(26)	673
2.1	32×48	0.1403	0.244(10)	0.3485(78)	3.972(23)	749
2.2	24×48	0.1350	0.5808(52)	0.6265(42)	3.7732(44)	860
2.2	24×48	0.1360	0.4909(92)	0.5450(75)	3.876(48)	350
2.2	24×48	0.1375	0.3164(61)	0.3796(41)	4.952(51)	795
2.2	32×64	0.1375	0.3237(55)	1144

β	$N_s \times N_t$	κ_A	$am_{PS,A}$	am_{gg}	w_0/a	N_{conf}
2.1	24×48	0.1680	0.877(11)	1.324(91)	1.3182(15)	320
2.1	24×48	0.1690	0.6803(97)	1.073(41)	1.6071(18)	302
2.1	24×48	0.1695	0.381(23)	0.637(67)	2.289(11)	314
2.2	24×48	0.1600	1.048(12)	187
2.2	24×48	0.1640	0.530(13)	0.593(44)	3.065(19)	331
2.2	24×48	0.1650	0.315(20)	0.410(28)	3.011(16)	320
2.2	24×48	0.1652	0.244(20)	0.316(34)	3.348(27)	333
2.2	32×64	0.1652	128

This table is a summary of the data of the pure adjoint ($\kappa_F = 0$) and pure fundamental ($\kappa_A = 0$) runs. The clover coefficient was set to the one-loop values of $C_{SW,F} = 1.297$ and $C_{SW,A} = 1.696$ at $\beta = 2.1$ ($C_{SW,F} = 1.283$ and $C_{SW,A} = 1.664$ at $\beta = 2.2$).

APPENDIX C: SUMMARY OF THE RUNS WITH TWO DYNAMICAL REPRESENTATIONS

β	$N_s \times N_t$	κ_A	κ_F	$amp_{PCAC,F}$	$amp_{PS,F}$	$af_{PS,F}$	$am_{V,F}$	$amp_{PCAC,A}$	$amp_{PS,A}$	$af_{PS,A}$	$am_{V,A}$	am_{gg}	w_0/a	N_{conf}
2.1	24 × 48	0.158	0.134	0.12160(11)	0.4775(37)	0.04330(34)	0.4955(36)	0.14217(21)	0.8047(52)	0.1673(13)	0.8661(68)	0.721(21)	...	850
2.1	24 × 48	0.160	0.134	0.110448(88)	0.4399(45)	0.04074(32)	0.4621(34)	0.08657(18)	0.5885(59)	0.1306(15)	0.6453(70)	0.535(25)	4.369(61)	480
2.1	24 × 48	0.162	0.134	0.09691(17)	0.3985(77)	0.03634(44)	0.4206(61)	0.02611(19)	0.270(12)	0.0697(18)	0.312(17)	0.261(24)	4.583(56)	304
2.1	24 × 48	0.100	0.135	0.18668(21)	0.8221(73)	0.0908(13)	0.8848(79)	1.23247(73)	2.9703(35)	0.2611(11)	2.9964(38)	2.54(18)	...	379
2.1	24 × 48	0.120	0.135	0.17354(29)	0.760(11)	0.0790(14)	0.8150(96)	0.89868(85)	2.4428(58)	0.3192(23)	2.4955(62)	2.156(60)	...	203
2.1	24 × 48	0.140	0.135	0.14713(28)	0.634(11)	0.0659(15)	0.6695(78)	0.53590(76)	1.815(11)	0.3350(63)	1.898(15)	1.52(11)	...	213
2.1	24 × 48	0.150	0.135	0.12226(11)	0.5238(56)	0.05152(59)	0.5519(44)	0.33084(29)	1.3672(67)	0.2854(40)	1.4529(97)	1.180(29)	...	473
2.1	24 × 48	0.155	0.135	0.10484(13)	0.4545(75)	0.04509(57)	0.4803(44)	0.21306(31)	1.0385(75)	0.2109(27)	1.10841(10)	0.867(25)	...	412
2.1	24 × 48	0.158	0.135	0.09178(10)	0.4093(43)	0.04156(35)	0.4396(32)	0.13628(17)	0.7805(50)	0.1624(16)	0.8418(63)	0.682(16)	3.274(20)	845
2.1	24 × 48	0.160	0.135	0.08039(18)	0.3521(67)	0.03684(41)	0.3960(52)	0.08063(26)	0.5578(81)	0.1220(17)	0.6183(91)	0.469(14)	3.711(24)	398
2.1	24 × 48	0.161	0.135	0.07379(13)	0.3260(76)	0.03706(45)	0.3527(63)	0.05136(22)	0.4240(94)	0.1009(15)	0.482(11)	0.426(17)	4.058(20)	302
2.1	24 × 48	0.162	0.135	0.06582(10)	0.3319(69)	0.03234(41)	0.3625(50)	0.01926(18)	0.230(11)	0.0665(14)	0.288(14)	0.214(19)	4.754(27)	318
2.1	24 × 48	0.158	0.136	0.06004(12)	0.2983(56)	0.03457(35)	0.3399(46)	0.12980(20)	0.7495(60)	0.1539(16)	0.8062(65)	0.668(22)	3.879(55)	754
2.1	32 × 48	0.158	0.136	0.06147(19)	0.3239(72)	0.03756(63)	0.3754(48)	849
2.1	24 × 48	0.160	0.136	0.04884(13)	0.2515(71)	0.03403(51)	0.3039(55)	0.07356(20)	0.5186(72)	0.1144(15)	0.5734(73)	0.411(15)	3.987(21)	572
2.1	24 × 48	0.161	0.136	0.04217(10)	0.2514(68)	0.02938(46)	0.3080(39)	0.04351(21)	0.3773(89)	0.0897(11)	0.438(10)	0.324(17)	4.368(39)	328
2.1	24 × 48	0.162	0.136	0.03426(14)	0.1988(86)	0.02939(49)	0.2479(54)	0.01242(25)	0.178(13)	0.0604(20)	0.265(15)	0.178(14)	4.615(35)	438
2.1	32 × 48	0.162	0.136	0.03467(11)	0.211(11)	0.02564(53)	0.2666(43)	0.01314(19)	0.1991(85)	0.0569(13)	0.2805(98)	0.217(16)	...	447
2.1	24 × 48	0.160	0.100	0.9927(14)	2.464(11)	0.1151(22)	2.478(11)	0.23826(55)	1.214(13)	0.3779(84)	1.422(25)	0.97(27)	...	150
2.1	24 × 48	0.160	0.120	0.49525(19)	1.4090(55)	0.07159(80)	1.4193(60)	0.1633(12)	0.951(30)	0.243(12)	1.050(43)	0.955(65)	...	303
2.1	24 × 48	0.160	0.132	0.16970(14)	0.6083(36)	0.04694(34)	0.6202(34)	0.09917(23)	0.6484(77)	0.1411(23)	0.711(90)	0.706(17)	4.18(12)	445
2.1	24 × 48	0.160	0.133	0.14080(11)	0.5230(50)	0.04516(38)	0.5452(37)	0.09281(20)	0.6181(76)	0.1389(17)	0.6813(85)	0.543(19)	3.855(43)	393
2.2	24 × 48	0.157	0.132	0.139759(85)	0.5019(48)	0.04121(40)	0.5215(40)	0.09512(16)	0.5802(72)	0.1137(17)	0.6322(83)	0.435(28)	4.127(43)	347
2.2	24 × 48	0.158	0.132	0.135202(62)	0.4901(33)	0.03879(31)	0.5020(29)	0.06658(17)	0.4582(94)	0.0918(16)	0.4893(99)	0.439(52)	4.921(15)	600
2.2	24 × 48	0.158	0.133	0.105987(74)	0.4141(41)	0.03564(28)	0.4355(32)	0.06197(17)	0.4340(59)	0.08687(96)	0.4787(59)	0.364(24)	5.299(47)	561
2.2	24 × 48	0.158	0.134	0.076362(91)	0.3393(73)	0.03281(36)	0.3854(45)	0.05777(20)	0.4134(79)	0.0880(15)	0.4688(80)	0.363(19)	4.639(25)	336
2.2	24 × 48	0.159	0.134	0.07203(10)	0.3363(68)	0.03281(40)	0.3784(53)	0.02901(24)	0.2883(83)	0.0734(12)	0.362(10)	0.309(23)	4.034(31)	362
2.2	24 × 48	0.158	0.135	0.045494(91)	0.2234(57)	0.03000(40)	0.2750(45)	0.05234(15)	0.3842(67)	0.0798(10)	0.4304(70)	0.317(25)	4.886(39)	536
2.2	24 × 48	0.159	0.135	0.039821(90)	0.2473(82)	0.02603(43)	0.2680(61)	0.02204(23)	0.2102(87)	0.05549(85)	0.264(12)	0.272(33)	5.561(50)	329
2.2	32 × 64	0.159	0.135	0.04338(17)	0.244(11)	0.03160(52)	0.3125(65)	0.02592(22)	0.2725(99)	0.0722(19)	0.364(10)	0.286(13)	...	338

This table summarizes the runs with two dynamical representations. The clover coefficient was again set to the one-loop values of $C_{sw,F} = 1.297$ and $C_{sw,A} = 1.696$ at $\beta = 2.1$ ($C_{sw,F} = 1.283$ and $C_{sw,A} = 1.664$ at $\beta = 2.2$).

- [1] T. DeGrand, M. Golterman, E. T. Neil, and Y. Shamir, *Phys. Rev. D* **94**, 025020 (2016).
- [2] V. Ayyar, T. DeGrand, M. Golterman, D. C. Hackett, W. I. Jay, E. T. Neil, Y. Shamir, and B. Svetitsky, *Phys. Rev. D* **97**, 074505 (2018).
- [3] V. Ayyar, T. DeGrand, D. C. Hackett, W. I. Jay, E. T. Neil, Y. Shamir, and B. Svetitsky, *Phys. Rev. D* **97**, 114505 (2018).
- [4] V. Ayyar, M. F. Golterman, D. C. Hackett, W. Jay, E. T. Neil, Y. Shamir, and B. Svetitsky, *Phys. Rev. D* **99**, 094504 (2019).
- [5] M. Golterman, W. I. Jay, E. T. Neil, Y. Shamir, and B. Svetitsky, [arXiv:2010.01920](https://arxiv.org/abs/2010.01920).
- [6] G. Cossu, L. Del Debbio, M. Panero, and D. Preti, *Eur. Phys. J. C* **79**, 638 (2019).
- [7] J. Giedt, *Int. J. Mod. Phys. A* **24**, 4045 (2009).
- [8] M. Costa and H. Panagopoulos, *Phys. Rev. D* **96**, 034507 (2017).
- [9] B. Wellegehausen and A. Wipf, Proc. Sci., LATTICE2018 (2018) 210.
- [10] G. Bergner and S. Piemonte, Proc. Sci., LATTICE2018 (2019) 209.
- [11] G. Cacciapaglia, C. Pica, and F. Sannino, *Phys. Rep.* **877**, 1 (2020).
- [12] L. Del Debbio, B. Lucini, A. Patella, C. Pica, and A. Rago, *Phys. Rev. D* **82**, 014510 (2010).
- [13] T. DeGrand, Y. Shamir, and B. Svetitsky, *Phys. Rev. D* **83**, 074507 (2011).
- [14] A. Patella, *Phys. Rev. D* **86**, 025006 (2012).
- [15] S. Aoki, I. H. Lee, and R. E. Shrock, *Phys. Lett. B* **219**, 335 (1989).
- [16] S. Aoki, I. H. Lee, and R. E. Shrock, *Phys. Lett. B* **207**, 471 (1988).
- [17] A. Athenodorou, E. Bennett, G. Bergner, and B. Lucini, *Phys. Rev. D* **91**, 114508 (2015).
- [18] G. Bergner, P. Giudice, G. Münster, P. Scior, I. Montvay, and S. Piemonte, *J. High Energy Phys.* **01** (2018) 119.
- [19] T. A. Ryttov and F. Sannino, *Phys. Rev. D* **78**, 115010 (2008).
- [20] T. A. Ryttov and R. Shrock, *Phys. Rev. D* **98**, 096003 (2018).
- [21] S. Girmohanta, T. A. Ryttov, and R. Shrock, *Phys. Rev. D* **99**, 116022 (2019).
- [22] R. Lewis, C. Pica, and F. Sannino, *Phys. Rev. D* **85**, 014504 (2012).
- [23] A. Hietanen, R. Lewis, C. Pica, and F. Sannino, *J. High Energy Phys.* **07** (2014) 116.
- [24] R. Arthur, V. Drach, M. Hansen, A. Hietanen, C. Pica, and F. Sannino, *Phys. Rev. D* **94**, 094507 (2016).
- [25] V. Drach, T. Janowski, and C. Pica, *EPJ Web Conf.* **175**, 08020 (2018).
- [26] R. C. Brower, A. Hasenfratz, C. Rebbi, E. Weinberg, and O. Witzel, *Phys. Rev. D* **93**, 075028 (2016).
- [27] A. Hasenfratz, C. Rebbi, and O. Witzel, *Phys. Lett. B* **773**, 86 (2017).
- [28] T. Appelquist *et al.* (Lattice Strong Dynamics), [arXiv:2007.01810](https://arxiv.org/abs/2007.01810).
- [29] G. Ferretti, *J. High Energy Phys.* **06** (2014) 142.
- [30] G. Bergner and S. Piemonte, *J. High Energy Phys.* **12** (2014) 133.
- [31] G. Bergner, S. Piemonte, and M. Ünsal, *J. High Energy Phys.* **11** (2018) 092.
- [32] A. Cherman, T. Schäfer, and M. Ünsal, *Phys. Rev. Lett.* **117**, 081601 (2016).
- [33] T. Kanazawa and M. Ünsal, *Phys. Rev. D* **102**, 034013 (2020).
- [34] S. Musberg, G. Münster, and S. Piemonte, *J. High Energy Phys.* **05** (2013) 143.
- [35] S. Catterall, J. Giedt, F. Sannino, and J. Schneible, *J. High Energy Phys.* **11** (2008) 009.
- [36] B. Lucini, A. Patella, A. Rago, and E. Rinaldi, *J. High Energy Phys.* **11** (2013) 106.
- [37] G. Münster and H. Stüwe, *J. High Energy Phys.* **05** (2014) 034.
- [38] G. Bergner, P. Giudice, I. Montvay, G. Münster, and S. Piemonte, *Eur. Phys. J. Plus* **130**, 229 (2015).
- [39] G. Bergner, P. Giudice, G. Münster, I. Montvay, and S. Piemonte, *J. High Energy Phys.* **03** (2016) 080.
- [40] N. Seiberg, *Nucl. Phys.* **B435**, 129 (1995).
- [41] L. Del Debbio and R. Zwicky, *Phys. Rev. D* **82**, 014502 (2010).
- [42] www.gauss-centre.eu.
- [43] www.lrz.de.